



HAL
open science

Regularized phase retrieval algorithms for X-ray phase tomography of 3D bone cell culture analysis

Loriane Weber, Max Langer, Peter Cloetens, Françoise Peyrin

► **To cite this version:**

Loriane Weber, Max Langer, Peter Cloetens, Françoise Peyrin. Regularized phase retrieval algorithms for X-ray phase tomography of 3D bone cell culture analysis. Medical Applications of Synchrotron Radiation MASR 2015, Oct 2015, Villard de Lans, France. hal-01236233

HAL Id: hal-01236233

<https://hal.science/hal-01236233v1>

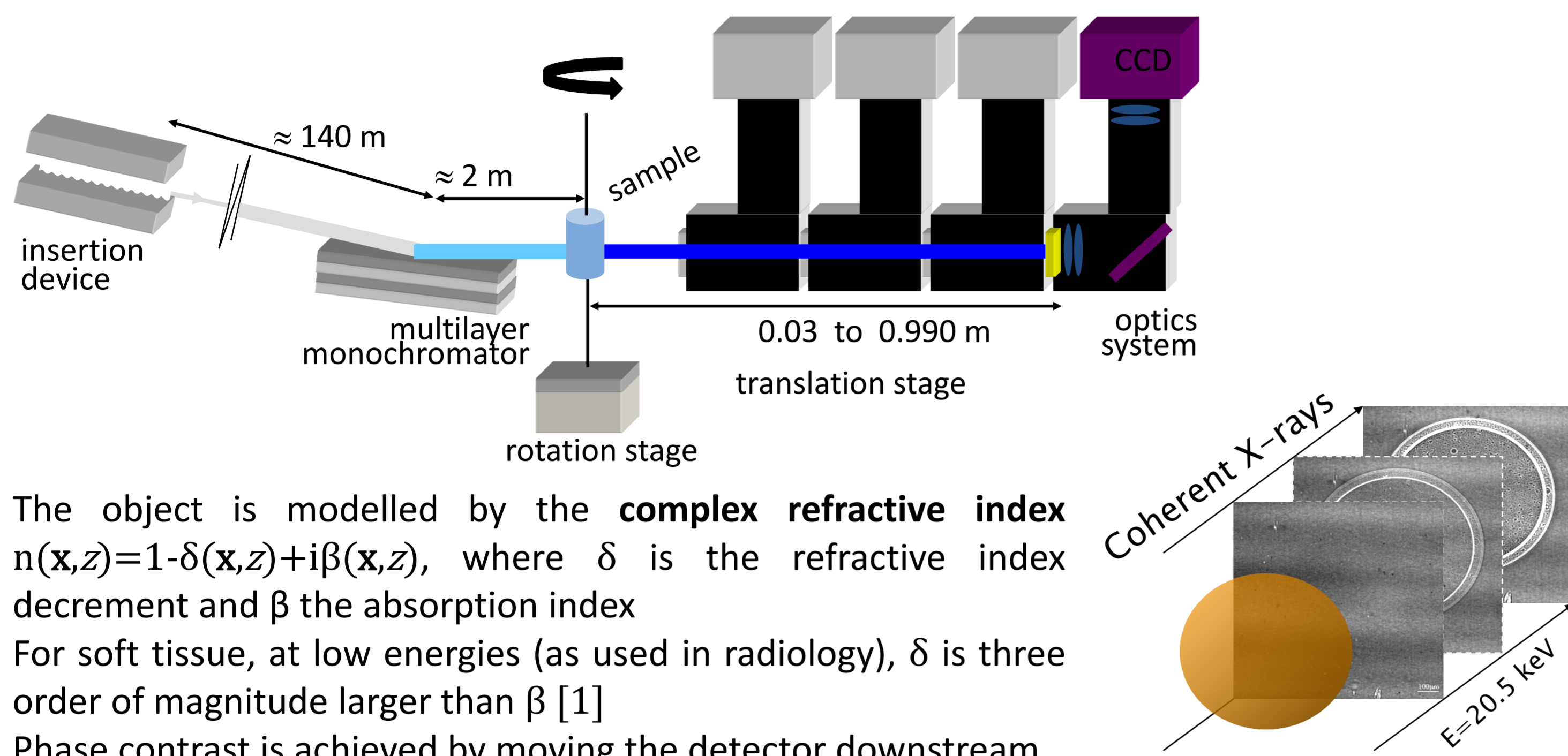
Submitted on 14 Nov 2018

HAL is a multi-disciplinary open access archive for the deposit and dissemination of scientific research documents, whether they are published or not. The documents may come from teaching and research institutions in France or abroad, or from public or private research centers.

L'archive ouverte pluridisciplinaire **HAL**, est destinée au dépôt et à la diffusion de documents scientifiques de niveau recherche, publiés ou non, émanant des établissements d'enseignement et de recherche français ou étrangers, des laboratoires publics ou privés.

In-line phase contrast tomography

Setup and image formation



- The object is modelled by the **complex refractive index** $n(\mathbf{x}, z) = 1 - \delta(\mathbf{x}, z) + i\beta(\mathbf{x}, z)$, where δ is the refractive index decrement and β the absorption index
- For soft tissue, at low energies (as used in radiology), δ is three order of magnitude larger than β [1]
- Phase contrast is achieved by moving the detector downstream
- Attenuation B and phase shift φ induced by the object described as projections perpendicular to the propagation direction \vec{z} (note that $\mathbf{x} = (x, y)$ represents the coordinates in the real domain and $\mathbf{f} = (f_x, f_y)$ the coordinates in the Fourier domain).

$$B(\mathbf{x}) = \frac{2\pi}{\lambda} \int \beta(\mathbf{x}, z) dz \quad \text{and} \quad \varphi(\mathbf{x}) = \frac{2\pi}{\lambda} \int \delta(\mathbf{x}, z) dz$$

- At each angle θ , the interaction between the object and the X-ray can be described as a transmittance function

$$T_{\theta}(\mathbf{x}) = \exp[-B_{\theta}(\mathbf{x}) + i\varphi_{\theta}(\mathbf{x})]$$

- The free space propagation over a distance D can be modelled by the Fresnel propagator P_D (**Fresnel diffraction**)

$$T_{\theta, D}(\mathbf{x}) = (T_{\theta} * P_D)(\mathbf{x})$$

- The intensity recorded by the detector at a distance D is

$$I_{\theta, D}(\mathbf{x}) = |T_{\theta, D}(\mathbf{x})|^2$$

- In **holotomography** [2], images are acquired at:
 - several source-to-sample distances
 - under different angles of rotations
- Phase projections** are obtained by combining these multi-distance projections for each angle θ using phase retrieval.

Image reconstruction

- A two-step process: phase retrieval and tomographic reconstruction
 - Phase retrieval:** calculate the phase shift $\varphi_{\theta}(\mathbf{x})$ from the phase contrast images at different propagation distances $\{I_{\theta, D}(\mathbf{x}), D = D_1 \dots D_n\}$
 - Ill-posed inverse problem, which requires regularization
 - Usually solved by least-square method
 - Tomographic reconstruction:** reconstruct the 3D refractive index image from the estimated phase shifts $\hat{\varphi}_{\theta}(\mathbf{x})$ at different projection angles θ
 - Usually solved by filtered back-projection (FBP).

Phase retrieval methods

- Least-square method (LSQ)**, based on the Contrast Transfer Function

$$\tilde{\varphi}(\mathbf{f}) = \frac{\sum_D \sin(\pi\lambda D |f|^2) [\tilde{I}_D(\mathbf{f}) - \delta_{Dirac}(\mathbf{f})]}{[\sum_D 2\sin^2(\pi\lambda D |f|^2)] + \alpha}$$
- Advanced regularized method ("quasi-iterative methods")**
 - $\hat{\varphi}_{\theta}(\mathbf{x}) = \arg \min_{\psi} \sum_D [|\tilde{I}_{\theta, D, \psi}(\mathbf{x}) - I_{\theta, D}(\mathbf{x})|^2 + \alpha |\psi_{\theta}(\mathbf{x}) - \psi_{\theta, 0}(\mathbf{x})|^2]$
 - Designing the prior

Homogeneous objects

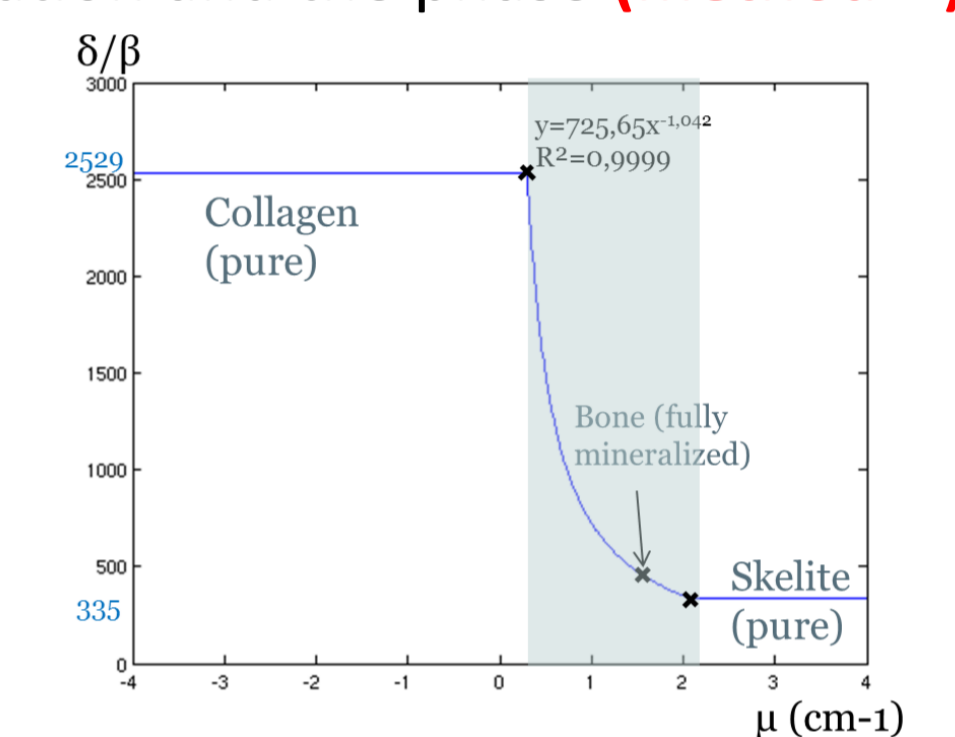
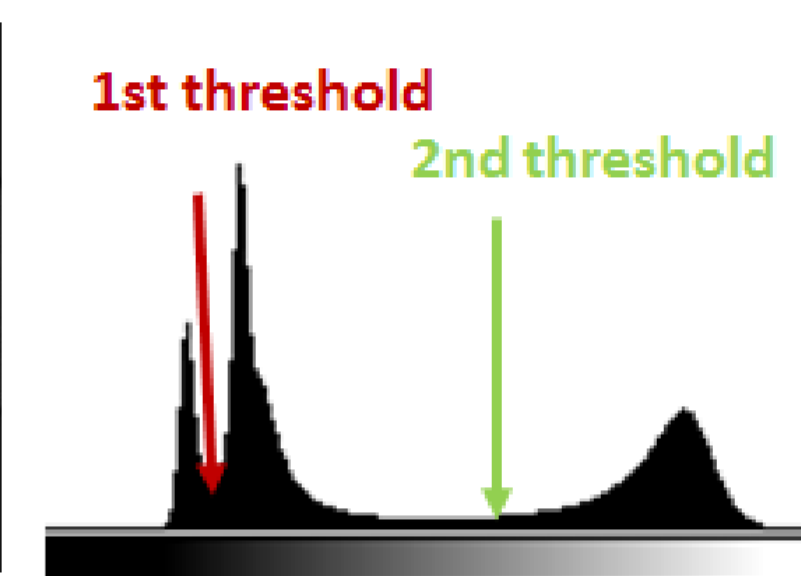
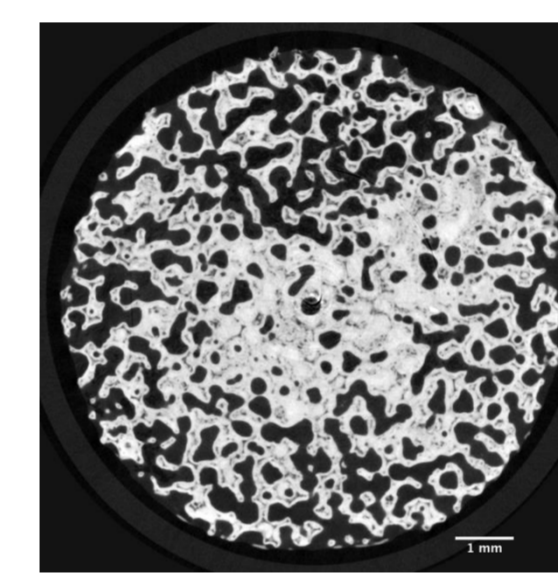
- Can be introduced in projections
- Paganin[3]:** proportionality between phase and attenuation (**method P**)

$$\varphi(\mathbf{x}) = -\frac{\delta}{2\beta} \ln \left(\mathcal{F}^{-1} \left\{ \frac{\mathcal{F}\{I_D(\mathbf{x})\}}{1 + \frac{\lambda D \delta}{4\pi\beta} \|f\|^2} \right\} \right)$$
- Langer[4]:** prior introduced in the regularization (**method A**)

$$\varphi_{\theta, 0}(\mathbf{x}) = f(\mathbf{x}) \frac{\delta}{2\beta} \ln [I_{\theta, D}(\mathbf{x})]$$

Heterogeneous objects

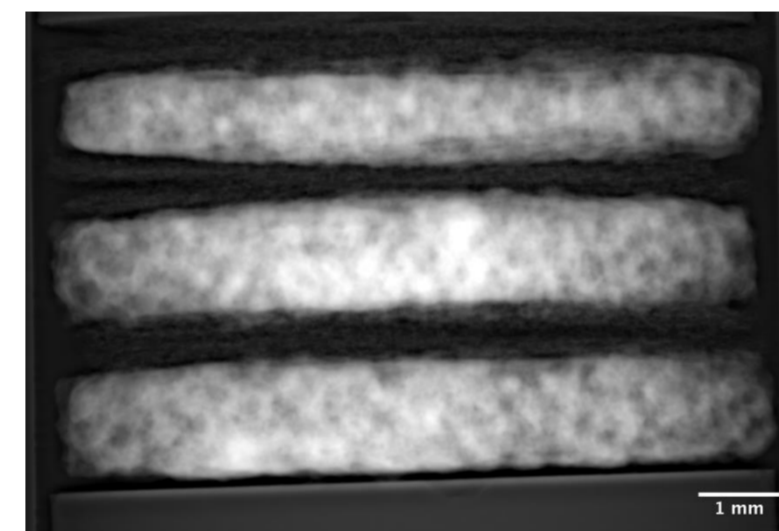
- Must be introduced in object domain
- Langer[5]:** Thresholding of the attenuation scan → **Bi-material object (methods B & C)**
- Langer[6]:** **Functional relationship** between the attenuation and the phase (**method D**)



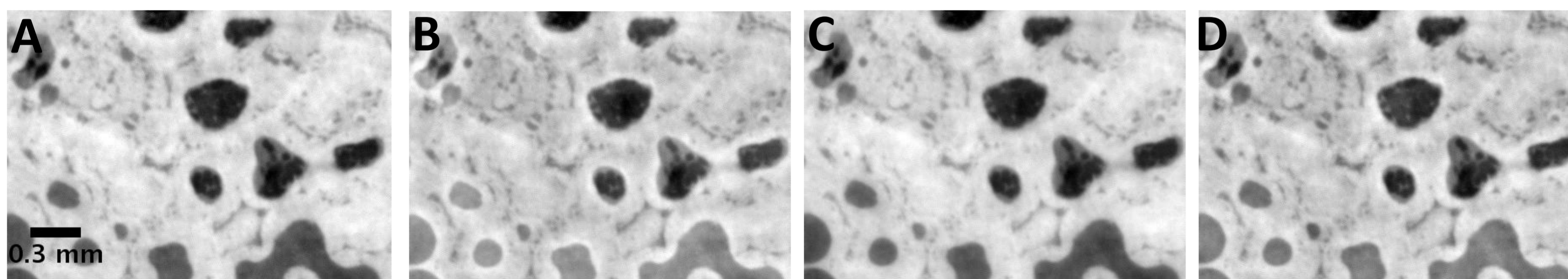
Application to 3D cell cultures

Material and methods

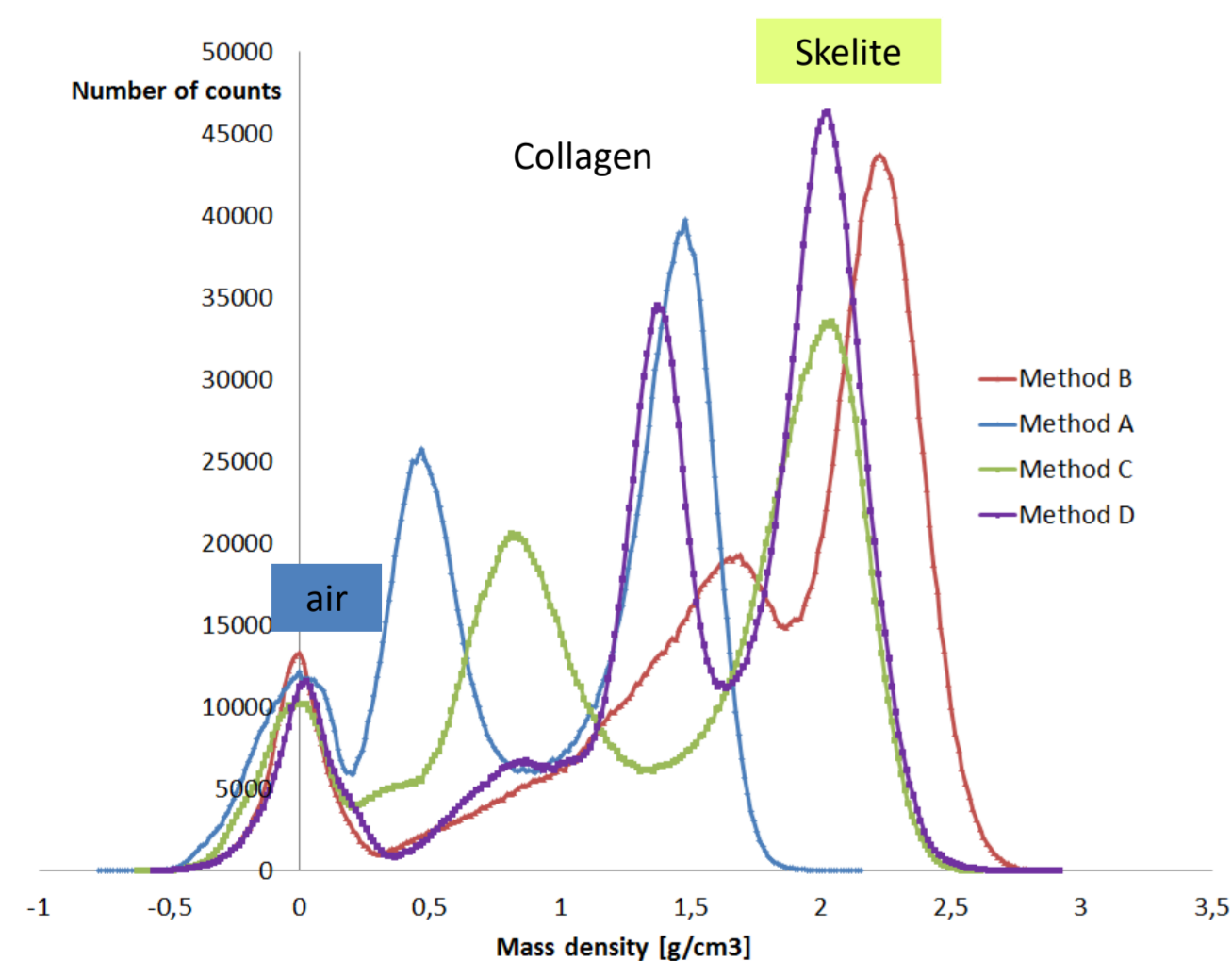
- Biomaterial (Skelite®) used for 3D cell culture and artificial bone scaffolds in surgery (coll. R Cancedda, University of Genova) [7]
- Composed of Si-TCP(67%) and β -TCP/HA (33%)
- 9 scaffolds imaged: discs of 9 mm diameter, seeded with bone cells
- Experimental conditions:** 2000 projections, 30 keV, 4 sample-to-detector distances, pixel size=5 μ m, Field of view = 10.2 mm
- Reconstruction methods:** see above



Results



Crop of a reconstructed slice, using homogeneous approach [A], heterogeneous approach with 1st threshold [B] or 2nd threshold [C], and heterogeneous approach with a functional relationship [D].

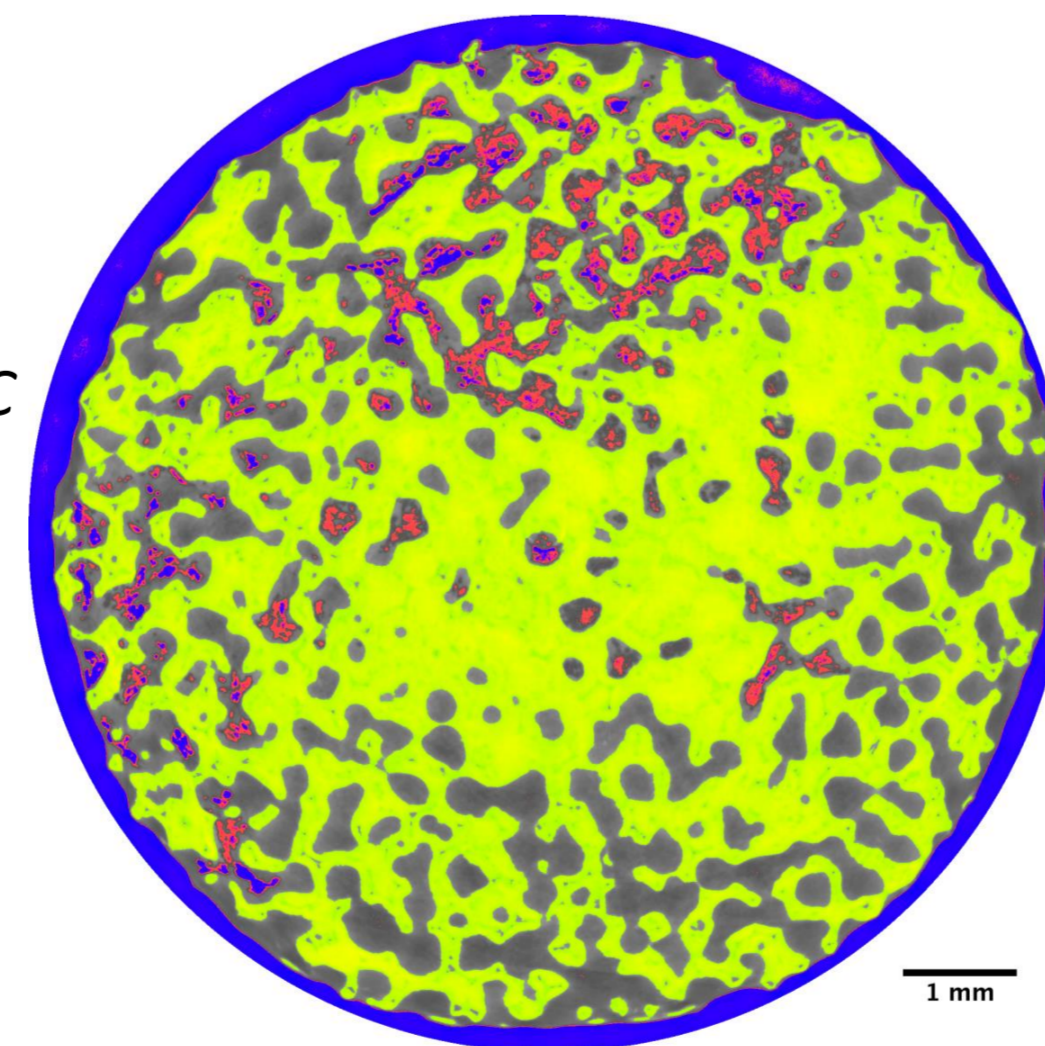


Histograms of volumetric mass densities of the reconstructed slice with the 4 methods

Theoretical vol. mass densities:

- $\rho(\text{air}) = 1.3 \times 10^{-3} \text{ g/cm}^3$
- $\rho(\text{Collagen}) = 1 \text{ g/cm}^3$
- $\rho(\text{Skelite}^{\circledR}) = 1.8 \text{ g/cm}^3$

Thresholded slice reconstructed with method C

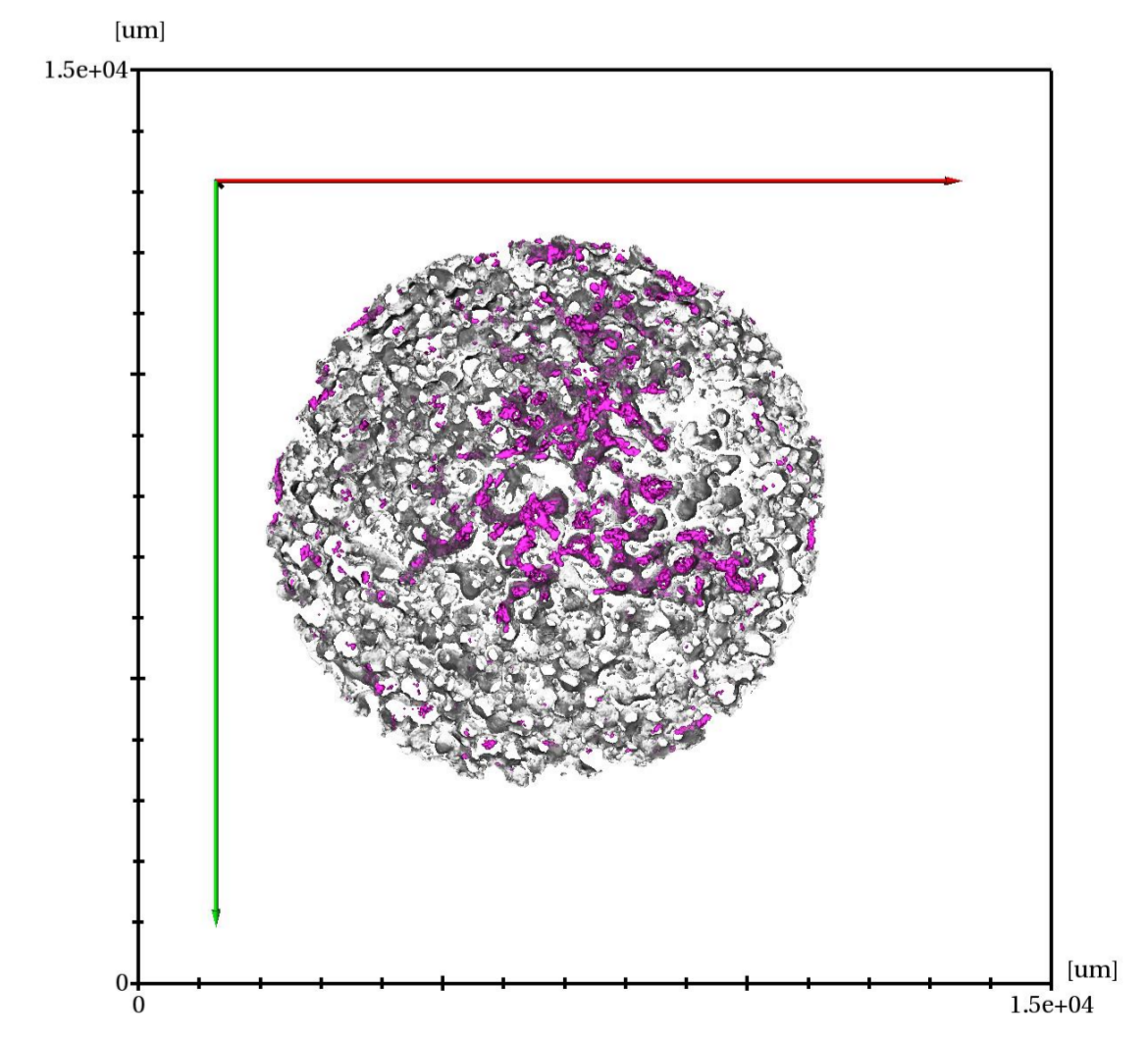
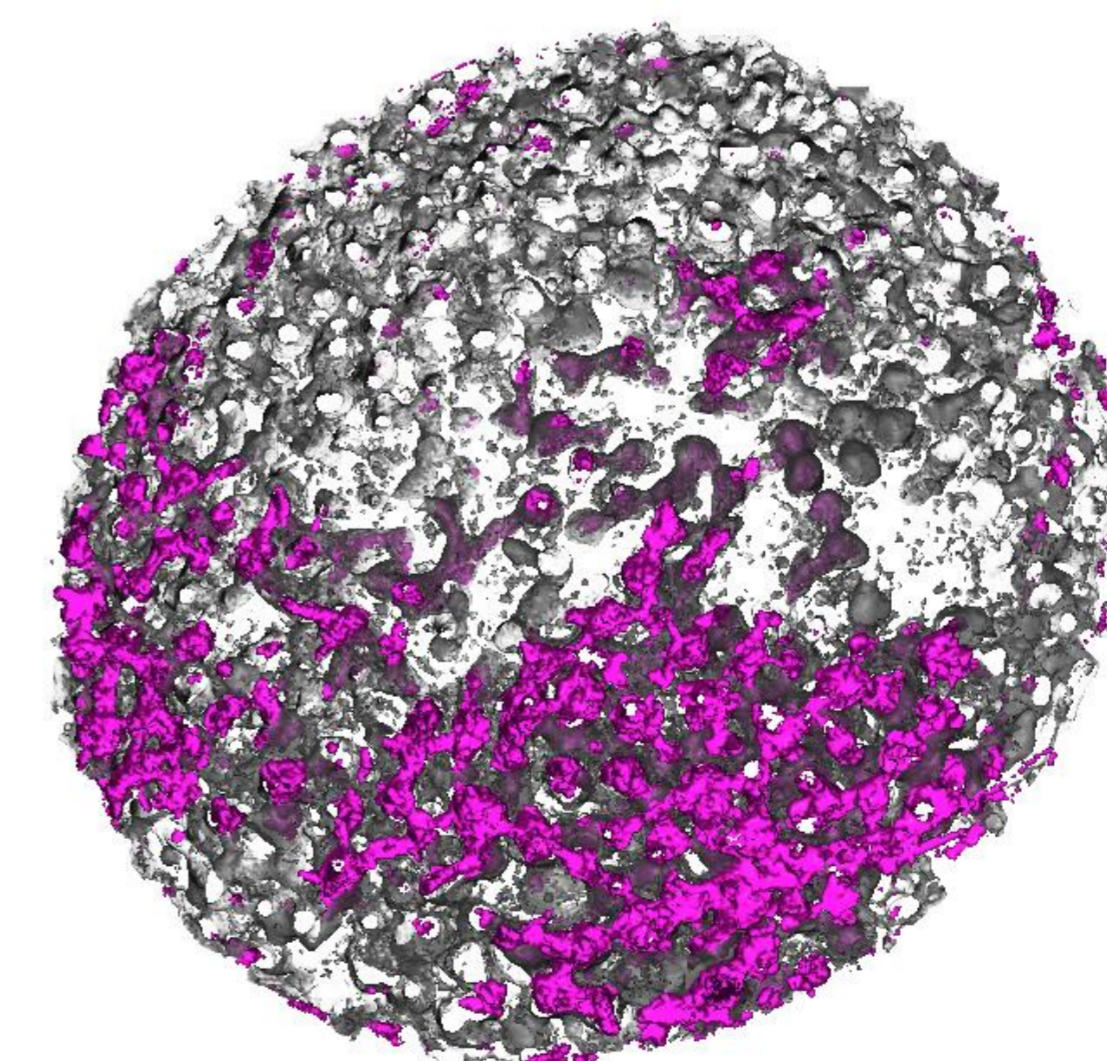


- Only 3 modes are visible using methods A and B, while we can distinguish 4 modes with methods C and D.
- Method A presents fringes around soft tissue, and phase contrast artefacts are visible using methods B and D.
- Method C seems more quantitative, and image quality is improved with regards to the other methods.

Statistical analysis

- 9 samples: 3 samples / type of seeded cells (OBs, pre-OCs, OBs+pre-OCs)
- Quantification of volumes and corresponding thicknesses: Mineralized Volume (MV), Immature bone Volume (IBV), volume of cells (C)
- ANOVA: whether there is a difference between the groups or not
- Tukey's HSD (honest significant difference): which groups are significantly different from each other.
- Statistical analysis showed no influence on seeded cells, except on the Immature Bone Volume.
- /!\ BUT: a very few samples imaged and analyzed.

Sample	Fraction (in %)			Local thickness (in μ m)		
	MV/TV	IBV/(TV-MV)	C/(TV-MV)	MV.Th	IBV.Th	C.Th
OBs	44,7 +/- 5,0	98,2 +/- 8,9	5,1 +/- 4,3	121,4 +/- 20,3	176,0 +/- 29,0	60,8 +/- 2,1
OBs + pre-OCs	46,4 +/- 1,9	91,7 +/- 14,3	0,45 +/- 0,60	123,66 +/- 20,27	206,23 +/- 43,38	64,71 +/- 26,26
pre-OCs	48,5 +/- 2,7	0 +/- 0	0 +/- 0	150,4 +/- 13,8	0 +/- 0	0 +/- 0



Conclusions & Perspectives

- Work to be submitted to *Phys. Med. Biol.*
- Heterogeneous object approaches can clearly improve image quality
- Choice of good parameters (threshold, function) is of crucial importance
- Introduce spatial constraints in prior, i.e. reconstruction while getting rid of the glass capillary
- Further quantitative studies using a calibrated phantom for example.

Acknowledgements

This work was supported by the LABEX PRIMES (ANR-11-LABX-0063) of Université de Lyon, within the program "Investissements d'Avenir" (ANR-11-IDEX-0007) operated by the French National Research Agency (ANR).